

Analysis and Quality of Service Evaluation of a Fast Charging Station for Electric Vehicles

Ioannis Zenginis^{a,*}, John S. Vardakas^a, Nizar Zorba^b, Christos V. Verikoukis^c

^a*Iquadrat, Barcelona, Spain*

^b*QMIC, Al-Doha, Qatar*

^c*Telecommunications Technological Centre of Catalonia (CTTC), Barcelona, Spain*

Abstract

1 Electrification of transportation is considered as one of the most promising
2 ways to mitigate climate change and reduce national security risks from oil and
3 gasoline imports. Fast Charging Stations (FCS) that provide high Quality of
4 Service (QoS) will facilitate the wide market penetration of Electric Vehicles
5 (EVs). In this paper, we analyze the operation of a FCS by employing a
6 novel queuing model. Our analysis considers that the various EV models
7 are divided into classes based on their battery size; then we compute the
8 EVs' mean waiting time in the queue, taking into account the number of
9 Charging Spots (CS) of the FCS, as well as the stochastic arrival process and
10 the stochastic recharging needs of the various EV classes. Furthermore, the
11 high precision of our analysis is confirmed through simulations. Therefore,
12 our model may be utilized by existing FCS operators that need to provide
13 high QoS, or by future investors for an efficient installation design.

Keywords:

electric vehicles, queuing theory, fast charging, quality of service

*Corresponding author

Email addresses: izenginis@iquadrat.com (Ioannis Zenginis),
jvardakas@iquadrat.com (John S. Vardakas), nizarz@qmic.com (Nizar Zorba),
cveri@cttc.es (Christos V. Verikoukis)

1. Introduction

The gradual replacement of Internal Combustion Engine (ICE) vehicles with EVs is highly promoted within the transportation sector [1] - [9]. A review of national targets can be found in [1], which forecasts an annual production of over 100 million vehicles by 2050. The main advantage of the EVs is their potential to reduce the dependence on fossil fuels, as well as the emissions caused by fuel combustion [2] - [4]. In addition, EVs may facilitate the integration of renewable energy systems into the grid [5] - [7].

On the other hand, the main concern over the EV technology is the confrontation of the drivers range anxiety problem, which refers to the EVs' short driving ranges and long charging durations. Therefore, the large deployment of FCSs is crucial in achieving the aforementioned ambitious targets [8], [9]. The Japanese standard CHAdeMO (CHAdEMO) is currently the most popular option for DC fast charging, while the Combined Coupler Standard (CCS) is an emerging technology being promoted by Europe Automotive Industry [10]. Many manufacturers such as Nissan, Mitsubishi and Kia [11] - [13] have equipped their EV models with the former technology, whereas other manufacturers such as BMW and Volkswagen use the latter [14], [15]. Furthermore, Electric Vehicle Supply Equipment (EVSE) manufacturers have designed CSs that contain both a CHAdEMO and a CCS outlet in a single cabinet [16].

For EVs, the role of FCSs will be similar to that of gasoline stations for ICE vehicles. FCSs provide high power rates and as a result, the duration of charging an EV battery up to 80% of its rated capacity ranges between 5 - 30 minutes [17]. This is a relatively short amount of time when compared

39 to the 6 - 8 hours needed using home equipment. However, fast charging
 40 duration is considered to be long when compared to the duration of refilling
 41 ICE vehicles (1 - 3 minutes). This may result in the formation of queues and
 42 long waiting times, especially during peak-traffic hours when the number of
 43 charging requests is expected to be high. In turn, long waiting times may
 44 cause EV drivers' discomfort and dissatisfaction. It is therefore essential for
 45 FCS operators to develop mechanisms for queue waiting time estimation,
 46 through the consideration of the EVs' stochastic arrival and charging times.

47 For the stochastic modeling of the EVs' charging process, various queuing
 48 theory models have been utilized, with M/M/s being the most common of
 49 them [18] - [26]. The advantage of this model is its simplicity, since the
 50 arrival process of the EVs is assumed to be Poisson (M), while the charging
 51 times of the EVs follow the exponential distribution (M). Finally, s denotes
 52 the number of CSs that the charging station facility contains. The main
 53 target of analysis [18] - [21] is the EVs' charging demand estimation. On the
 54 other hand, other studies in the literature target the improvement of QoS
 55 in charging stations, through the development of control strategies for the
 56 minimization of the EVs' waiting time. These strategies are applied either
 57 to a single charging station ([22]) or to a network of charging stations ([23] -
 58 [26]). In [27], the M/M/s/c queue is used for modeling a parking lot where
 59 c denotes the waiting room and s the available CSs. This model considers
 60 the maximum number of EVs that can be in the parking lot at the same
 61 time, either being charged or waiting in the queue. The QoS metrics in this
 62 case are both the queue waiting time and the blocking probability i.e. the
 63 probability that an EV will not enter the parking lot due to lack of waiting

space. A similar model ($M/M/s/s$) is used in a series of studies [28] - [32]. In these cases it is considered that there is no waiting room for the EVs, and hence blocking probability is the only QoS metric. A more flexible model is employed in [33] where the EVs' charging times are generally distributed ($M/G/\infty$). Nevertheless, no QoS metrics are considered in this model since the number of CSs is infinite.

In this paper, we model a FCS as a multiclass $M/G/s$ queuing system in order to derive the mean waiting time of the EVs in the queue. Similar to the aforementioned studies, the proposed analysis considers that the arrival process of the EVs is Poisson, where the EVs are served according to the First In First Out (FIFO) discipline. However, a key advantage of our model, compared to the state of the art, is that we adopt a more holistic approach for the determination of the EVs' charging time distribution; we take into account that the charging time of the EVs is a function of the energy they obtain during a fast charging session i.e. the size of their battery, the State of Charge (SoC) of their battery upon their arrival in the FCS, and the SoC of their battery upon their departure from the FCS. Moreover, we divide the EVs into classes taking into account the different battery capacities of the various EV models.

The determination of the mean waiting time in the queue is based on the steady state solution of the multiclass $M/G/s$ system. An approximate method for the derivation of the steady state solution of a single-class $M/G/s$ system is provided in [34]. Single-class consideration (i.e. a system where all EVs have the same battery type) entails a single value for the mean arrival rate of the Poisson process, as well as independent and identically distributed

89 random service times. This is not the case in our model where the EVs are
 90 considered to have different types of batteries (multiclass). In a multiclass
 91 system the mean arrival rates of the various EV classes are different, while the
 92 charging times of the EVs are not identically distributed random variables. A
 93 key point in the analysis of the multiclass M/G/s system is the aggregation
 94 of all EV classes into a single class, in order to obtain a superposed arrival
 95 process and a superposed charging time distribution. The analysis of a single-
 96 server multiclass M/G/1 system with a FIFO queue discipline is presented in
 97 [35]. Furthermore, the concept of multi-server multiclass M/G/s systems has
 98 been examined in several studies considering various priority queue disciplines,
 99 other than FIFO [36] - [38]. However, to the best of our knowledge, it is the
 100 first time that a multi-server multiclass M/G/s queuing system is handled
 101 considering a FIFO discipline.

102 The accuracy of the proposed analysis is verified through simulations and
 103 found to be completely satisfactory. An additional advantage of the proposed
 104 analytical model is its pattern-agnostic nature, since the various features of
 105 the system (EV classes, arrival rates, arrival and departure SoC, number of
 106 CSs) are considered in a parametric way. To this end, we derive the EVs'
 107 maximum arrival rates subject to a maximum allowed QoS satisfaction value
 108 for the waiting time. Furthermore, we propose a charging strategy that can
 109 enable the FCS operator serve a higher number of EVs, while at the same
 110 time providing the same QoS level. In both cases we also derive the operator's
 111 mean revenue.

112 This paper is organized as follows. In Section 2, we present the FCS
 113 architecture and the analysis of the multiclass M/G/s queue for the derivation

of the EVs' mean waiting time in the queue. In Section 3, we derive the upper bound of the EVs' arrival rates given a corresponding upper bound for the waiting time. The charging strategy that allows the FCS operator to accommodate even greater arrival rates is formulated in Section 3 as well. Section 4 is the evaluation section, where both analytical and simulation results are presented and discussed. We conclude in Section 5.

2. FCS Architecture and Analysis

We consider a FCS that is located in an urban area and consists of s CSs. Each CS contains both a CHAdeMO and a CCS outlet that provide the same power rate P_{CS} . Furthermore, each CS is able to provide service to only one EV at a time, since the two outlets cannot operate simultaneously [16]; therefore, in the case where all CSs are occupied, an arrived EV has to wait in the same queue, regardless its fast charging option (CHAdeMO or CCS).

The EVs are divided into C classes depending on the rated capacity of their batteries; an EV that belongs to the c^{th} class has a battery capacity of B_c . Class c EVs arrive at the FCS by following a Poisson process with mean arrival rate λ_c . Furthermore, their charging time T_c is directly proportional to the energy they obtain during a charging session E_c and inversely proportional to the CSs' power rate P_{CS} (Eq. (1)):

$$T_c = \frac{E_c}{P_{CS}} = (SoCD_c - SoCA_c) \frac{B_c}{P_{CS}} = (0.8 - SoCA_c) \frac{B_c}{P_{CS}} \quad (1)$$

where $SoCD_c$ is the state of charge of the battery upon the EVs' departure and $SoCA_c$ is the state of charge of the battery upon the EVs' arrival. The derivation of the charging time T_c is based on the assumption of a

constant power rate P_{CS} [17]. Furthermore, all EVs are considered to recharge their batteries up to $SoCD_c = 0.8$, which is the maximum possible value during a fast charging session [17]. On the other hand, $SoCA_c$ is considered to be a random variable that follows a Probability Distribution Function (PDF) $f_c(x) = P(SoCA_c = x)$ and a corresponding Cumulative Distribution Function (CDF) $F_c(x) = P(SoCA_c \leq x)$. Based on (1) and the aforementioned considerations, the charging time T_c of c -class EVs is also a random variable. The CDF, the PDF and the mean of T_c are derived by the following relations, respectively:

$$\begin{aligned} G_c(t) &= P(T_c \leq t) = P[(0.8 - SoCA_c) \frac{B_c}{P_{CS}} \leq t] = \\ &= P(SoCA_c > 0.8 - \frac{P_{CS}}{B_c} t) = 1 - F_c(x_c(t)) \end{aligned} \quad (2)$$

$$g_c(t) = \frac{d}{dt} G_c(t) \quad (3)$$

$$m_c = \int t g_c(t) dt \quad (4)$$

where $x_c(t) = 0.8 - (P_{CS}/B_c)t$. It should be noted that in a multiclass queuing system the product $a_c = \lambda_c m_c$ denotes the load of c -class EVs.

The determination of the mean waiting time of the EVs in the queue is based on the derivation of the superposed arrival process, the superposed charging time distribution and the total load of the system. This procedure is based on the aggregation of all C classes into a single class [35]. The superposed arrival procedure is determined as a Poisson process, since the arrival process of each EV class is Poisson ([39]); therefore, the mean superposed

155 arrival rate is:

$$\lambda = \sum_{c=1}^C \lambda_c \quad (5)$$

156 while the total load of the system equals to the sum of the loads of each class
157 [39]:

$$a = \sum_{c=1}^C a_c \quad (6)$$

158 The system's total load a represents the mean number of busy CSs in the
159 steady state [40], while a_c represents the mean number of CSs occupied by
160 c -class EVs.

161 In the next step we derive the analytical expression of the superposed
162 charging time distribution as follows. Let T be a random variable that
163 denotes the charging duration at an arbitrary CS, given that an EV of any
164 class enters for service. The probability that a c -class EV enters for service
165 at the aforementioned CS is [35]:

$$k_c = \frac{\lambda_c}{\lambda}. \quad (7)$$

166 As a result, the CDF of T $G(t)=P(T \leq t)$ is equivalent to the probability
167 $[k_1P(T_1 \leq t) \cup k_2P(T_2 \leq t) \cup \dots \cup k_CP(T_C \leq t)]$. The events $k_cP(T_c \leq t)$ are
168 mutually exclusive (only one EV is being charged at a time in the arbitrary
169 CS), hence $G(t)$ is determined by:

$$G(t) = \sum_{c=1}^C k_c G_c(t). \quad (8)$$

170 The expression of the CDF can be used for the determination of the PDF,

171 the mean and the variance of T through the following relations, respectively:

$$g(t) = \frac{d}{dt}G(t) \quad (9)$$

$$m = \int t g(t) dt \quad (10)$$

$$v = \int t^2 g(t) dt - m^2 \quad (11)$$

174 In addition, the following ratio defines the utilization rate of a multi-server
175 queuing system:

$$\rho = \frac{\lambda m}{s}. \quad (12)$$

176 It should be noted that a necessary condition for a stable queuing system
177 (have a finite queue in steady state) is $\rho < 1$ [40].

178 The derivation of the superposed arrival rate and charging time distribution
179 enables the simplification of the considered multiclass system into a single-
180 class M/G/s system. Consequently, the mean waiting time W of the EVs
181 in the queue can be determined by using the analysis presented in [34], by
182 assuming that $\rho < 1$. Initially, we calculate the mean number of customers
183 waiting in the queue in a single-class M/G/s system, $L_{M/G/s}$. This number is
184 approximated by [34]:

$$L_{M/G/s} \approx \frac{1 + c_v^2}{\frac{2c_v^2}{L_{M/M/s}} + \frac{1 - c_v^2}{L_{M/D/s}}} \quad (13)$$

185 where $L_{M/M/s}$ and $L_{M/D/s}$ are the mean number of customers waiting in the
186 queue in the corresponding M/M/s and M/D/s systems, respectively, while

187 c_v^2 is the square of the coefficient of variation of the service time PDF:

$$c_v^2 = \frac{v}{m^2}. \quad (14)$$

188 The mean number $L_{M/M/s}$ of customers waiting in the queue in an M/M/s
189 system is obtained by [40] :

$$L_{M/M/s} = \frac{\rho \alpha^s}{s!(1-\rho)^2} \left[\sum_{r=0}^{s-1} \frac{\alpha^r}{r!} + \frac{\alpha^s}{s!} \left(1 - \frac{\alpha}{s}\right)^{-1} \right]^{-1} \quad (15)$$

190 while $L_{M/D/s}$ is approximated using the following equations [34]:

$$L_{M/D/s} \approx \psi(s, \rho) L_{M/M/s} \quad (16)$$

191

$$\psi(s, \rho) = \frac{1}{2} \left[1 + \Phi(\theta) \zeta(\rho) \left(1 - \exp \left\{ -\frac{\theta}{\Phi(\theta) \zeta(\rho)} \right\} \right) \right] \quad (17)$$

192

$$\zeta(\rho) = \frac{1-\rho}{\rho} \quad (18)$$

193

$$\Phi(\theta) = \frac{\theta}{8(1+\theta)} \left(\sqrt{\frac{9+\theta}{1-\theta}} - 2 \right), \text{ with } \theta = \frac{s-1}{s+1} \quad (19)$$

194 Finally, the mean number $L_{M/G/s}$ of customers waiting in the queue in the
195 single-class M/G/s system is used for the determination of the mean waiting
196 time of customers (EVs) in the queue through Little's law [40]:

$$W = \frac{L_{M/G/s}}{\lambda}. \quad (20)$$

197 3. QoS satisfaction and proposed charging strategy

198 The main advantage of public FCSs compared to slow charging at home
199 is the short charging duration, due to the high power rates they provide.
200 However, for a FCS to provide high QoS, the EVs' waiting time in the queue
201 should be kept to low levels; otherwise, the aforementioned advantage is
202 pointless. In this section we initially compute the EVs' maximum arrival
203 rates, so as the mean waiting time in the queue equals to a maximum limit
204 W_q . Next, given the aforementioned QoS criterion, we propose a charging
205 strategy that can be implemented by the FCS operator, in order to increase
206 the maximum arrival rate capacity of the system. Moreover, in both cases,
207 we compute the operator's mean revenue during a time interval τ , by taking
208 into account that the EVs' mean arrival rates are equal to their maximum
209 values during the interval τ .

210 The mean waiting time of the EVs in the queue depends on the superposed
211 arrival rate and the superposed charging time distribution of the system. In
212 turn, the superposed charging time distribution is derived based on the
213 charging time distribution of each single class, as well as on the probabilities
214 k_c . In this analysis we assume that the values of k_c can be approximated
215 based on the market shares h_c of the EV classes in the region where the FCS
216 is located, so that $k_c=h_c$. The aforementioned consideration allows for the
217 computation of the maximum superposed arrival rate λ_{\max} and the maximum
218 arrival rate of each EV class, $\lambda_{c,\max}$ by using Algorithm 1. Algorithm 1
219 uses as input parameters the QoS criterion for the waiting time, the battery
220 capacities, the $SoCA_c$ PDFs and the market shares of the EV classes, as
221 well as the number of CSs and the power rate they provide. At the first

222 stage it derives the charging time distribution of each class and the system's
 223 superposed charging time distribution. The second stage refers to a loop
 224 that calculates the maximum superposed arrival rate using the waiting time
 225 upper limit as a termination condition. Finally, Algorithm 1 determines the
 226 maximum arrival rate of each class based on the result of stage 2 and the
 227 probabilities k_c .

Algorithm 1

INPUT: The QoS criterion W_q , a set of EV classes $(B_c, h_c, f_c(x))$, the number of CSs s and their power rate P_{CS} .

for $j=1$ to C **do**

$k_c(j)=h_c(j)$

 calculate $G_c(j, t)$ through Eq. (2).

end for

Calculate $G(t)$, $g(t)$, m and c_v through Eqs. (8), (9), (10) and (14), respectively.

Initialize: $\lambda_{max} = 1$, $W = 0$.

while $(W \leq W_q)$ **do**

 calculate W through Eqs. (12)-(20)

$\lambda_{max} = \lambda_{max} + 0.0001$

end while

for $j=1$ to C **do**

$\lambda_{c,max}(j) = \lambda_{max} k_c(j)$

end for

228 Next, we calculate the operator's mean revenue R during a time interval
 229 τ . We assume that during this interval the arrival rates are equal to their
 230 maximum values. Furthermore, we consider that the duration τ is long enough
 231 so as the queuing system reaches steady state. The aforementioned concept
 232 may represent a peak traffic period during a typical day. As it is noticed
 233 in Section 2, the total load of the system represents the mean number of

234 occupied CSs in steady state. Hence, the mean power drawn by the EVs P_{EVs}
 235 during the interval τ is given by the product of the mean number of occupied
 236 CSs, $a_{\max} = \lambda_{\max} m$ by the power rate of each CS, P_{CS} :

$$P_{EVs} = a_{\max} P_{CS} \quad (21)$$

237 Furthermore, the mean energy that is supplied to the EVs during the interval
 238 τ is:

$$E_{EVs} = \tau P_{EVs} \quad (22)$$

239 Finally, the mean revenue R of the operator is calculated in (23) where r
 240 ($\text{€}/\text{kWh}$) denotes the price that the FCS operator charges the served EVs.

$$R = r E_{EVs} \quad (23)$$

241 We now proceed with the formulation of a charging strategy, according
 242 to which the FCS operator provides financial incentives (price discount) to
 243 those EVs that accept to recharge their batteries up to an arranged departure
 244 SoC threshold $SoCD_{thr} < 0.8$. The objective of the proposed strategy is to
 245 enable the FCS operator to increase the maximum arrival rate capacity i.e.
 246 $\lambda'_{\max} > \lambda_{\max}$ while providing the same QoS level. For the derivation of the
 247 maximum arrival rates λ'_{\max} and $\lambda'_{c,\max}$, in this case, we divide each single class
 248 into two additional subclasses c_1 and c_2 . Subclass c_1 contains the percentage
 249 σ_c of c -class EVs that accept the operator's offer, hence, $k_{c1} = \sigma_c k_c$. On the
 250 contrary, subclass c_2 contains the remaining $1 - \sigma_c$ percentage of c -class EVs
 251 that do not accept the operator's offer, hence, $k_{c2} = (1 - \sigma_c) k_c$. The charging

252 time CDF $G_{c1}(t)$ and PDF $g_{c1}(t)$, as well as the mean charging time m_{c1} for
 253 the EVs belonging to subclasses c_1 , $c = (1, 2, \dots, C)$ are derived through Eqs.
 254 (2) - (4), respectively, by replacing $x_c(t)$ with:

$$x_{c1}(t) = SoCD_{thr} - \frac{P_{CS}}{B_c}t. \quad (24)$$

Algorithm 2

INPUT: The QoS criterion W_q , a set of EV classes $(B_c, h_c, f_c(x), \sigma_c)$, the number of CSs s and their power rate P_{CS} , as well as the departure SoC threshold $SoCD_{thr}$.

for $j=1$ to C **do**

$k_c(j)=h_c(j)$

$k_{c1}(j)=\sigma_c h_c(j)$

$k_{c2}(j)=(1-\sigma_c)h_c(j)$

 calculate $G_{c1}(j, t)$ through Eqs. (2) and (24)

 calculate $G_{c2}(j, t)$ through Eq. (2).

end for

Calculate $G(t)$, $g(t)$, m and c_v through Eqs. (8), (9), (10) and (14), respectively.

Initialize: $\lambda'_{max} = 1$, $W = 0$.

while ($W \leq W_q$) **do**

 calculate W through Eqs. (12)-(20)

$\lambda'_{max} = \lambda'_{max} + 0.0001$

end while

for $j=1$ to C **do**

$\lambda'_{c,max}(j) = \lambda'_{max} k_c(j)$

end for

255 Regarding the charging time CDF $G_{c2}(t)$, the PDF $g_{c2}(t)$ and the mean
 256 m_{c2} of the EVs belonging to subclasses c_2 , they have exactly the same form
 257 as in the set of Eqs. (2) - (4). Based on the aforementioned analysis,
 258 the maximum arrival rates λ'_{max} and $\lambda'_{c,max}$, under the proposed charging

strategy, are computed using Algorithm 2. Note that compared to Algorithm 1, Algorithm 2 uses two extra input parameters i.e. σ_c and $SoCD_{thr}$.

The operator's mean revenue R' under the proposed charging strategy is calculated by:

$$R' = \tau P_{CS} (1 - d) r \sum_{c=1}^C a_{c1} + \tau P_{CS} r \sum_{c=1}^C a_{c2}. \quad (25)$$

As it is noticed in Section 2, the load of each class (or subclass) represents the mean number of CSs occupied by the EVs that belong to this class (or subclass). Under the proposed strategy the load of subclasses c_1 is $a_{c1} = \sigma_c \lambda'_{c,\max} m_{c1}$ while the load of subclasses c_2 is $a_{c2} = (1 - \sigma_c) \lambda'_{c,\max} m_{c2}$, with $c = (1, 2, \dots, C)$. Note also that the EVs which belong to subclasses c_2 are charged with r , while the EVs that belong to subclasses c_1 are offered a discount d i.e. $r' = (1 - d)r$. Therefore, the first product in Eq. (25) represents the operator's mean revenue due to the energy supplied to the EVs that belong to subclasses c_1 , while the second product represents the operator's mean revenue due to the energy supplied to the EVs that belong to subclasses c_2 .

4. Evaluation

In this section, we provide analytical and simulation results for the evaluation of the proposed modeling of a FCS as a multiclass M/G/s system. To this end, we consider a FCS that consists of $s=5$ CSs. A detailed description of the technical specifications of these CSs is provided in [16]. Based on [16], the power rate of both CHAdeMO and CCS outlets is $P_{CS}=50$ kW. Furthermore,

280 the multiclass M/G/s system consists of $C=3$ EV classes which correspond
 281 to 3 of the most popular EV models of the Spanish market [41]; namely,
 282 Nissan Leaf ($B_1=24\text{kWh}$), BMW i3 ($B_2=18.8\text{ kWh}$) and Mitsubishi i-MiEV
 283 ($B_3=16\text{ kWh}$). We also consider that the random variables SoCA_1 , SoCA_2
 284 and SoCA_3 follow the normal PDF with mean 0.25 and standard deviation
 285 0.059. The value of the standard deviation has been selected such that the
 286 interval $[0.15, 0.4]$ to be the 95% confidence interval of the PDF; the selection
 287 of the aforementioned PDF is based on the assumption that the vast majority
 288 of the EVs seek for fast charging facilities when their batteries' SoC ranges
 289 between 0.15 and 0.4.

290 The evaluation of the proposed analysis is performed through the compar-
 291 ison of analytical results with corresponding results from simulation. To this
 292 end, we built a simulator using Matlab, which considers the aforementioned
 293 FCS architecture, while it creates events (EV arrivals and departures) based
 294 on random numbers. In order to simulate the Poisson arrival process, the
 295 simulator considers a large number of EV arrivals i.e. 10^6 . For each simulated
 296 EV, we record the time of its arrival, the time of its entering for charging
 297 and the time of its departure from a CS, in order to determine the EVs'
 298 mean waiting time in the queue. Simulation results that are presented in
 299 this Section are obtained as mean values of 20 runs. It should be noted that
 300 the analytical results are obtained through the proposed analytical model in
 301 less than 0.2 sec., which is a significantly shorter time compared to 12 min.,
 302 required in average for a single simulation run.

303 Analytical and simulation results for the mean waiting time in the queue
 304 versus the superposed arrival rate of the system are presented in Fig. 1. For

Table 1: Parameters for the 3 evaluation scenarios.

| Scenario | k_1 | k_2 | k_3 | m (h) |
|----------|-------|-------|-------|---------|
| 1 | 0.5 | 0.25 | 0.25 | 0.2277 |
| 2 | 0.25 | 0.5 | 0.25 | 0.2134 |
| 3 | 0.25 | 0.25 | 0.5 | 0.2057 |

the derivation of the waiting-time results, we consider 3 different scenarios regarding the values of the probabilities k_c . For each scenario, Table 1 summarizes the set of values for k_c and the system's mean charging time, which is calculated through Eq. (10). Scenario 1 considers that the arrival rate of Leaf (class 1), which is the EV model with the biggest battery, is twice the arrival rates of i3 (class 2) and i-MiEV (class 3). On the other hand, scenario 3 considers that the arrival rate of i-MiEV, which is the EV model with the smallest battery, is twice the arrival rates of the other EV models. For this reason, scenario 1 is characterized by the longest mean charging time, while scenario 3 is characterized by the shortest one.

As Fig. 1 indicates, despite the different mean charging time values under the 3 scenarios, the performance of the system is quite similar for arrival rate values up to 14 (EVs/hour). After that point, the waiting time shows a sharper rise with the increase of λ . This can be interpreted by mapping the arrival rate values to utilization rate values through Eq. (9). The waiting time curve becomes steeper as the utilization rate of the system approaches its limiting value i.e. 1. This tendency is more intense under scenario 1, which is the scenario with the highest mean charging time. Finally, it should also be pointed out that the comparison of analytical and simulation results of Fig. 1 reveals that the accuracy of our model is very satisfactory; in all cases

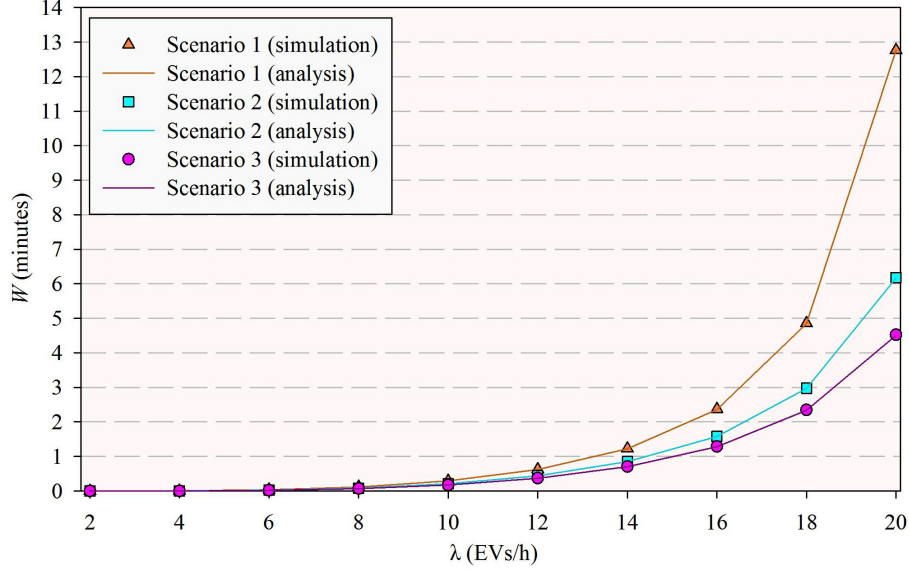


Figure 1: Waiting-time results for the 3 evaluation scenarios.

the difference between analysis and simulation is smaller than 1%.

Next, we compute the maximum arrival rates of the EVs given that the mean waiting time in the queue is equal to a maximum allowed for QoS satisfaction limit $W_q=1$ min. For the derivation of the ratios k_c in this case, we take into account market data [41]. For example, dividing the population of Leaf by the aggregate population of the 3 EV models, we derive that $k_1=0.543$. Following the same process for i3 and i-MiEV, k_2 and k_3 are found to be 0.133 and 0.324, respectively. One of the main contributions of this study is the derivation of the superposed charging time distribution $g(t)$. Fig. 2 presents the charging time distribution of each class and the superposed charging time distribution of the whole system. By using Algorithm 1, the maximum value for the superposed arrival rate is found to be $\lambda_{max}=13.37$ (EVs/h) while the corresponding maximum arrival rates of each class are found to be $\lambda_{1,max}=7.26$ (EVs/h), $\lambda_{2,max}=1.78$ (EVs/h) and $\lambda_{3,max}=4.33$

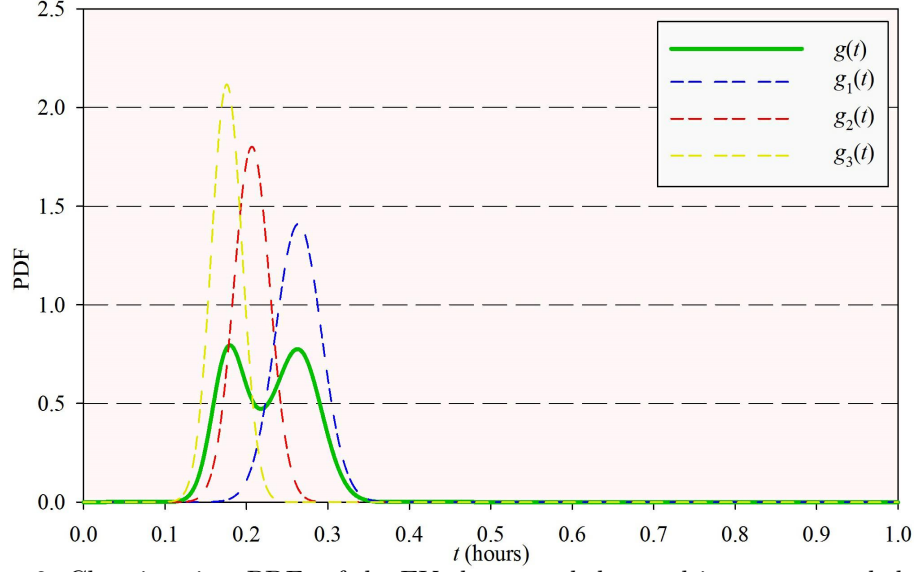


Figure 2: Charging time PDFs of the EV classes and the resulting superposed charging time PDF of the whole system.

339 (EVs/h). Assuming that the operator's energy tariff is $r=0.15$ (€/kWh), as
 340 well as that the arrival rates are equal to their maximum values during a
 341 period of $\tau=4$ h, the revenue of the operator during this period is $R=91.4$
 342 €(Eq. 23).

343 In what follows, we investigate the FCS operator's capability to increase the
 344 maximum arrival rate capacity of the system by $\gamma = \lambda'_{\max}/\lambda_{\max}$, while keeping
 345 the same QoS level. This can be achieved by implementing the charging
 346 strategy proposed in Section 3. Crucial for the effectiveness of the charging
 347 strategy are the values of parameters σ_c , $c = (1, 2, 3)$ which determine the
 348 percentage of the EVs that belong to subclasses c_1 . Fig. 3 presents analytical
 349 results of the parameter γ versus the percentages σ_c . For presentation purposes
 350 we assume that $\sigma_1=\sigma_2=\sigma_3=\Sigma$. Furthermore, we evaluate the performance
 351 of the proposed strategy by considering two departure SoC thresholds (0.65

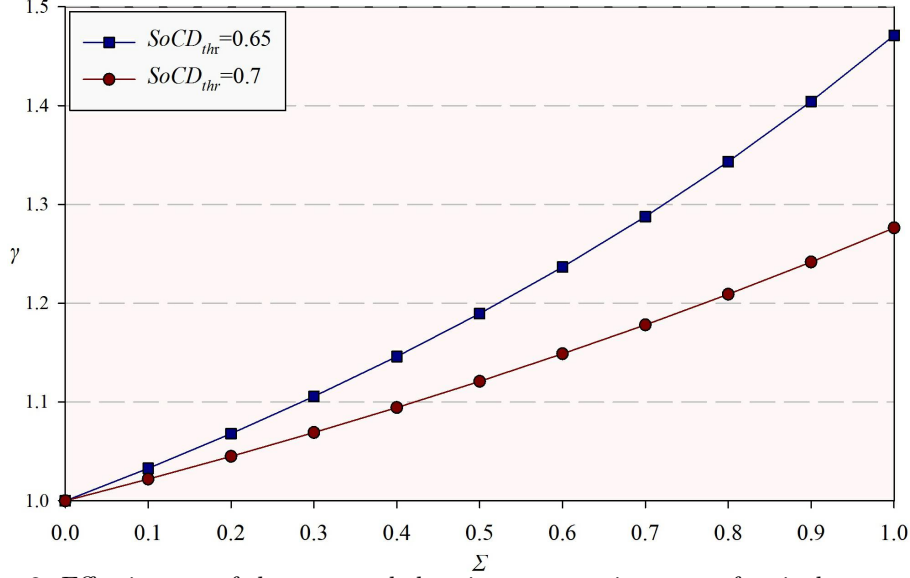


Figure 3: Effectiveness of the proposed charging strategy in terms of arrival rate capacity increase.

and 0.7, respectively). As it was anticipated, parameter γ increases with the increase of Σ . This is due to the fact that the EVs that belong to subclasses c_1 obtain less amount of energy than the EVs of subclasses c_2 . Hence, the greater the values of Σ , the shorter the mean charging time of the system becomes. As a result, the capability of the FCS operator to serve greater arrival rates providing the same QoS level increases. Furthermore, the EVs of subclasses c_1 obtain less energy when $SoCD_{thr}=0.65$ compared to the case where $SoCD_{thr}=0.7$. Hence, for the same values of Σ , the performance of the proposed strategy is better in the $SoCD_{thr}=0.65$ case.

The proposed charging strategy dictates that the operator makes a discount d to those EVs that accept to recharge up to an arranged departure SoC level lower than 0.8 (i.e. 0.7 and 0.65 in our evaluation examples). Fig. 4 presents the maximum discount d_{max} that the operator is able to make versus the

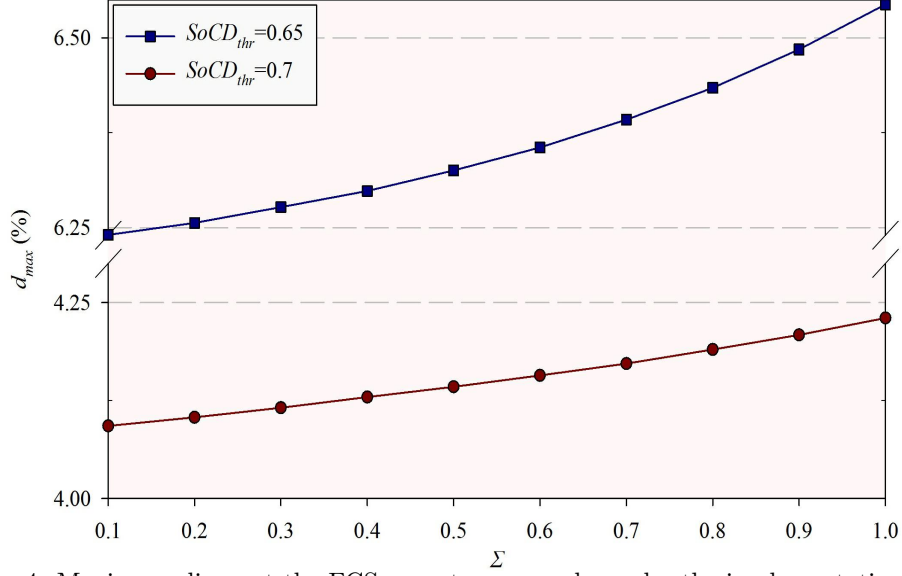


Figure 4: Maximum discount the FCS operator can make under the implementation of the proposed charging strategy.

parameter Σ . The values of d_{max} are obtained by setting $R'=R$ and solving for d . Note that R is calculated through Eq. (23) and represents the revenue of the operator during a period where all EVs recharge up to $SoCD=0.8$ and the arrival rates are equal to λ_{max} . R' is calculated through Eq. (25) and represents the revenue of the operator during the same period; however in the latter occasion a percentage of EVs (Σ) recharge up to $SoCD_{thr}$, while the arrival rates are equal to λ'_{max} .

Let us compare the case where all EVs ($\Sigma=100\%$) recharge up to $SoCD_{thr}=0.7$ with the case where all EVs recharge up to $SoCD=0.8$. In the former case each EV obtains less energy than in the latter. However, the total amount of energy that the operator provides is higher in the first case than in the second due to the increase in the EVs' maximum arrival rates (by $\gamma=1.28$, Fig. 3). As a result, the operator can make a discount $d_{max}=4.23\%$ (Fig.

4) in the price that sells energy without financial losses. It is reasonable to assume that the EV drivers would more easily accept to recharge their batteries up to $SoCD_{thr}=0.7$ instead of $SoCD_{thr}=0.65$. However, as Fig. 4 shows, the FCS operator can make the $SoCD_{thr}=0.65$ case more attractive by providing greater discounts. Finally, Fig. 4 also indicates that the operator's capability to make a greater discount increases with the amount (Σ) of the EVs that accept the offer. This is attributed to the fact that higher values of Σ correspond to higher maximum arrival rates (Fig.3).

5. Conclusion

We present and analyze the operation of a FCS for EVs as a multiclass M/G/s system. The various EV models are divided into classes depending on their battery capacity, while the charging time distribution of the EVs that belong to the same class is derived based on the amount of energy they obtain during a fast charging session. The proposed analytical model considers the arrival rate and the charging time distribution of each class, and determines the expected waiting time of the EVs in the queue. Simulation results verify the accuracy of our analysis. The EVs' waiting time is the QoS metric of our study. To this end, we also provide an algorithm that uses as input parameters an upper bound for the waiting time, as well as the market share of the various EV models, and outputs the upper bound of the EVs' arrival rates. Note that the aforementioned algorithm considers that the EVs recharge their batteries up to the maximum possible SoC level (0.8). Then, we propose a charging strategy to increase the maximum arrival rate capacity. The proposed strategy considers that the EVs are provided with

402 financial incentives, in order to recharge their batteries up to a departure
403 SoC threshold lower than 80%. The effectiveness of the proposed strategy
404 depends on the departure SoC level which is arranged by the operator, as
405 well as the amount of the EVs that accept the operator's offer. Finally, our
406 developed model allows for the calculation of the operator's mean revenue.

407 References

- 408 [1] T. Trigg, P. Telleen, Global EV Outlook - Understanding the Electric
409 Vehicle landscape to 2020, Tech. Rep.
- 410 [2] M. Densing, H. Turton, G. Bäuml, Conditions for the successful deploy-
411 ment of electric vehicles - A global energy system perspective, *Energy*
412 47 (1) (2012) 137 – 149.
- 413 [3] W. J. Smith, Can EV (electric vehicles) address Ireland's CO2 emissions
414 from transport?, *Energy* 35 (12) (2010) 4514 – 4521.
- 415 [4] A. Colmenar-Santos, D. Borge-Diez, P. M. Ortega-Cabezas, J. Míguez-
416 Camiña, Macro economic impact, reduction of fee deficit and profitability
417 of a sustainable transport model based on electric mobility. Case study:
418 City of León (Spain), *Energy* 65 (2014) 303 – 318.
- 419 [5] B. S. M. Borba, A. Szklo, R. Schaeffer, Plug-in hybrid electric vehicles as
420 a way to maximize the integration of variable renewable energy in power
421 systems: the case of wind generation in northeastern Brazil, *Energy*
422 37 (1) (2012) 469 – 481.

- 423 [6] S. Bellekom, R. Benders, S. Pelgröm, H. Moll, Electric cars and wind
424 energy: Two problems, one solution? A study to combine wind energy
425 and electric cars in 2020 in The Netherlands, *Energy* 45 (1) (2012) 859 –
426 866.
- 427 [7] Q. Zhang, B. C. Mclellan, T. Tezuka, K. N. Ishihara, A methodology for
428 economic and environmental analysis of electric vehicles with different
429 operational conditions, *Energy* 61 (2013) 118 – 127.
- 430 [8] P. Sadeghi-Barzani, A. Rajabi-Ghahnavieh, H. Kazemi-Karegar, Optimal
431 fast charging station placing and sizing, *Applied Energy* 125 (2014) 289 –
432 299.
- 433 [9] L. Zhang, B. Shaffer, T. Brown, G. S. Samuelson, The optimization of
434 DC fast charging deployment in California, *Applied Energy* 157 (2015)
435 111 – 122.
- 436 [10] M. C. Falvo, D. Sbordone, M. Devetsikiotis, et al., EV charging stations
437 and modes: international standards, in: *IEEE SPEEDAM*, IEEE, 2014,
438 pp. 1134 – 1139.
- 439 [11] <http://www.nissanusa.com/electric-cars/leaf/>, [Online; Accessed
440 15 October 2015].
- 441 [12] <http://www.mitsubishicars.com/imiev>, [Online; Accessed 15 October
442 2015].
- 443 [13] <http://www.kia.com/eu/future/soul/>, [Online; Accessed 15 October
444 2015].

- 445 [14] <http://www.bmw.com/com/en/newvehicles/i/i3/2013/showroom/>,
446 [Online; Accessed 15 October 2015].
- 447 [15] <http://www.volkswagen.co.uk/new/e-up-nf/home>, [Online; Accessed
448 15 October 2015].
- 449 [16] [https://www.chargepoint.com/files/Efeccec-QC-50-DC-fast-](https://www.chargepoint.com/files/Efeccec-QC-50-DC-fast-charger-datasheet.pdf)
450 [charger-datasheet.pdf](https://www.chargepoint.com/files/Efeccec-QC-50-DC-fast-charger-datasheet.pdf), [Online; Accessed 15 October 2015].
- 451 [17] H. Hoimoja, A. Rufer, G. Dziechciaruk, A. Vezzini, An ultrafast ev
452 charging station demonstrator, in: Proc. IEEE SPEEDAM, 2012, pp.
453 1390 – 1395.
- 454 [18] R. Garcia-Valle, J. G. Vlachogiannis, Letter to the editor: electric vehicle
455 demand model for load flow studies, Electric Power Components and
456 Systems 37 (5) (2009) 577–582.
- 457 [19] S. Bae, A. Kwasinski, Spatial and temporal model of electric vehicle
458 charging demand, IEEE Trans. Smart Grid 3 (1) (2012) 394–403.
- 459 [20] H. Liang, I. Sharma, W. Zhuang, K. Bhattacharya, Plug-in electric
460 vehicle charging demand estimation based on queueing network analysis,
461 in: Proc. IEEE PES Gen. Meet., Washington, 2014, pp. 1 – 5.
- 462 [21] G. Li, X.-P. Zhang, Modeling of plug-in hybrid electric vehicle charging
463 demand in probabilistic power flow calculations, IEEE Trans. Smart Grid
464 3 (1) (2012) 492 – 499.
- 465 [22] Q. Gong, S. Midlam-Mohler, E. Serra, V. Marano, G. Rizzoni, PEV

- charging control for a parking lot based on queuing theory, in: Proc. ACC 2013, 2013, pp. 1124 – 1129.
- [23] S.-N. Yang, W.-S. Cheng, Y.-C. Hsu, C.-H. Gan, Y.-B. Lin, Charge scheduling of electric vehicles in highways, *Math. Comp. Model.* 57 (11) (2013) 2873–2882.
- [24] H. Qin, W. Zhang, Charging scheduling with minimal waiting in a network of electric vehicles and charging stations, in: Proc. 8th ACM Int. Worksh. Vehicular Inter-Netw., Las Vegas, USA, 2011, pp. 51–60.
- [25] D. Said, S. Cherkaoui, L. Khoukhi, Queuing model for EVs charging at public supply stations, in: Proc. IWCMC, 2013, pp. 65–70.
- [26] A. Gusrialdi, Z. Qu, M. Simaan, et al., Scheduling and cooperative control of electric vehicles’ charging at highway service stations, in: Proc. 53rd IEEE CDC, 2014, pp. 6465–6471.
- [27] C. Farkas, L. Prikler, Stochastic modelling of EV charging at charging stations, in: Proc. ICREPQ, 2012, pp. 28–30.
- [28] G. Michailidis, M. Devetsikiotis, S. Bhattacharya, A. Chakraborty, F. Granelli, et al., Local energy storage sizing in plug-in hybrid electric vehicle charging stations under blocking probability constraints, in: Proc. IEEE SmartGridComm, 2011, pp. 78–83.
- [29] G. Michailidis, I. Papapanagiotou, M. Devetsikiotis, et al., Decentralized control of electric vehicles in a network of fast charging stations, in: Proc. IEEE Globecom, 2013, pp. 2785–2790.

- 488 [30] M. Ismail, M. Abdallah, K. Qaraqe, E. Serpedin, et al., A pricing-
489 based load shifting framework for EV fast charging stations, in: IEEE
490 SmartGridComm, 2014, pp. 680–685.
- 491 [31] I. Safak Bayram, M. Abdallah, K. Qaraqe, Providing QoS guarantees
492 to multiple classes of EVs under deterministic grid power, in: Proc.
493 ENERGYCON, 2014, pp. 1403–1408.
- 494 [32] J. S. Vardakas, Electric vehicles charging management in communication
495 controlled fast charging stations, in: Proc. IEEE CAMAD, 2014, pp.
496 115–119.
- 497 [33] M. Alizadeh, A. Scaglione, J. Davies, K. S. Kurani, A scalable stochastic
498 model for the electricity demand of electric and plug-in hybrid vehicles,
499 IEEE Trans. Smart Grid 5 (2) (2014) 848 – 860.
- 500 [34] T. Kimura, Approximations for multi-server queues: system interpola-
501 tions, Queueing Systems 17 (3 - 4) (1994) 347 – 382.
- 502 [35] N. Gautam, Analysis of queues: methods and applications, CRC Press,
503 2012.
- 504 [36] A. Federgruen, H. Groenevelt, M/G/c queueing systems with multiple
505 customer classes: characterization and control of achievable performance
506 under nonpreemptive priority rules, Management Science 34 (9) (1988)
507 1121 – 1138.
- 508 [37] M. Harchol-Balter, T. Osogami, A. Scheller-Wolf, A. Wierman, Multi-
509 server queueing systems with multiple priority classes, Queueing Systems
510 51 (3 - 4) (2005) 331 – 360.

- 511 [38] A. Al Hanbali, E. Alvarez, M. Heijden, Approximations for the waiting
512 time distribution in an M/G/c priority queue.
- 513 [39] H. Akimaru, K. Kawashima, Teletraffic Theory and Applications (1993).
- 514 [40] U. N. Bhat, An introduction to queueing theory: modeling and analysis
515 in applications, Springer Science & Business Media, 2008.
- 516 [41] [http://www.motorpasion.com/otros/ventas-en-espana-de-coches-](http://www.motorpasion.com/otros/ventas-en-espana-de-coches-y-furgonetas-electricas-en-2014)
517 [y-furgonetas-electricas-en-2014](http://www.motorpasion.com/otros/ventas-en-espana-de-coches-y-furgonetas-electricas-en-2014), [Online; Accessed 15 October
518 2015].